Optics Letters

High quality factor subwavelength grating waveguide micro-ring resonator based on trapezoidal silicon pillars

Zheng Wang,[1,2,†] Xiaochuan Xu,[3,†] Donglei Fan,[1,4] Yaguo Wang,[1,4] and Ray T. Chen[1,2,3,*]

[1]Materials Science and Engineering Program, Texas Materials Institute, The University of Texas at Austin, Austin, Texas 78712, USA
[2]Department of Electrical and Computer Engineering, The University of Texas at Austin, 10100 Burnet Rd., MER 160, Austin, Texas 78758, USA
[3]Omega Optics, Inc., 8500 Shoal Creek Blvd., Bldg. 4, Suite 200, Austin, Texas 78757, USA
[4]Department of Mechanical Engineering, The University of Texas at Austin, Austin, Texas 78712, USA
*Corresponding author: raychen@uts.cc.utexas.edu

Received 24 May 2016; revised 19 June 2016; accepted 21 June 2016; posted 23 June 2016 (Doc. ID 266690); published 15 July 2016

Subwavelength grating waveguide-based micro-ring resonators (SWGMRs) are a promising platform for research in light–matter interaction. However, it is extremely difficult to achieve small radius SWGMR devices (e.g., 5 μm) with satisfying quality factors (e.g., ~10,000). One major issue is the large bend loss of small radius SWGMRs. In this work, we report the use of trapezoidal silicon pillars instead of conventional rectangular silicon pillars as building blocks of SWGMRs. We found that an asymmetric effective refractive index profile created by trapezoidal silicon pillars can significantly reduce the bend loss and therefore increase the quality factors of SWGMRs. For the first time to the best of our knowledge, we have experimentally demonstrated a 5 μm radius SWGMR made of trapezoidal silicon pillars (T-SWGMR) with an applicable quality factor as high as 11,500, 4.6 times of that (~2800) offered by a conventional SWGMR made of rectangular silicon pillars, which indicates an 81.4% reduction of the propagation loss. This approach can also be readily employed to enhance SWGMRs with larger radii. We have also experimentally demonstrated a 10 μm radius T-SWGMR with a quality factor as high as 45,000, which indicates a propagation loss as low as 6.07 dB/cm.

OCIS codes: (050.6624) Subwavelength structures; (230.3120) Integrated optics devices.

http://dx.doi.org/10.1364/OL.41.003375

In recent decades, integrated photonics devices have attracted intensive research interest due to the great potential in realizing low cost photonic chips with well-established complementary metal–oxide semiconductor (CMOS) manufacturing technology [1–5]. Particularly, micro-ring resonators on the silicon-on-insulator (SOI) platform have been considered as basic building blocks for a vast range of applications [6]. Numerous photonic devices based on micro-ring resonators such as filters [7–9], switches [10–12], modulators [13–16], and sensors [17–19] have been demonstrated. However, conventional strip waveguide-based micro-ring resonators suffer from the intrinsic dilemma in having high quality factors but strong light-matter interactions with the environment. Specifically, a high quality factor requires a high light confinement for the desired low loss propagation, while the high light confinement also suggests a limited light-matter interaction, which jeopardizes the performance of the photonic devices built with micro-ring resonators. Recently, subwavelength grating (SWG) waveguides, comprised of periodically interleaved high and low refractive index materials with a pitch less than one wavelength, have been demonstrated as a promising solution to the aforementioned dilemma [20,21]. For SWG waveguides built on SOI wafers, the ratio of silicon and cladding materials (air, water, polymer, silicon dioxide, etc.) can be engineered microscopically to achieve the desired macroscopic properties. A precise control of these properties could potentially lead to significant improvements of photonic devices. Compared with photonic devices made of conventional strip waveguide-based micro-ring resonators, the ones built with SWG waveguide-based micro-ring resonators (SWGMRs), such as filters [22] and sensors [23], have shown promising improvements in performances. Nevertheless, the reported SWGMRs can only provide a moderate quality factor (~5600) even from a large radius of 15 μm [23], with which it is arduous to build practical compact photonics devices. It is highly desirable to investigate an approach for obtaining high quality factor SWGMRs with small radii.

According to the time-domain coupled-mode theory [24], the (loaded) quality factor Q of an SWGMR can be expressed as $1/Q = 1/Q_0 + 1/Q_c$ [25], where Q_0 is the intrinsic quality factor of an unloaded SWGMR, and Q_c is the coupling quality factor, which is defined as $Q_c = \omega_r/|\kappa|^2$. Here, ω_r is the resonance frequency, and κ is the coupling factor, which describes the coupling strength between the SWGMR and the adjacent bus waveguide. Once $Q_0 = Q_c$, the critical coupling is triggered, and Q reaches its maximum value at $Q = Q_0/2 = Q_c/2$. Although one can readily reduce the coupling strength via enlarging the gap between the SWGMR and the adjacent bus waveguide to increase Q_c, to achieve a high quality factor SWGMR, it is essential to increase Q_0. For a

small radius SWGMR, the large bend loss is one of the primary factors limiting its Q_0 [6]. In this Letter, we propose and experimentally demonstrate that the bend loss can be drastically reduced by exploiting trapezoidal silicon pillars instead of conventional rectangular silicon as building blocks of SWGMRs.

The 3D schematic of a conventional SWG waveguide built with rectangular silicon pillars is shown in Fig. 1(a), where Λ is the period of the SWG structure. l, w, and h represent the length, width, and height of the silicon pillars, respectively. In this study, SU-8 ($n = 1.58$) is selected as the top cladding material. The period Λ is 300 nm, and a typical silicon pillar with a geometry of $l \times w \times h = 150\ \text{nm} \times 500\ \text{nm} \times 250\ \text{nm}$ is selected. Quasi-transverse electric (TE) polarization is investigated in this study while the results can also be readily extended to quasi-transverse magnetic (TM) polarization. Theoretically lossless Bloch modes can exist in SWG waveguides. According to the effective medium theory (EMT), an SWG waveguide can be approximated as a uniform strip waveguide with an equivalent refractive index. Thus, similar to a strip waveguide, if the propagating optical mode still maintains the plane wave front in the curved region, photons need to travel faster as we move away from the center of the SWGMR. The speed of the wave front must exceed the speed of light at some points, the locus of which is known as radiation caustic [26]. Thus, the wave front must become curved beyond the radiation caustic. The curved wave front implies the occurrence of radiation, which causes mode leakage and energy loss. Theoretical analysis and numerical simulations based on the effective index method [27] and conformal transformation [28] unveil that the radiation induced bend loss has roots in the intrinsic distortion of the effective refractive index profile in an SWGMR. Thus, if a pre-distortion compensation of the effective refractive index profile could be made in an SWGMR, the aforementioned intrinsic distortion can be minimized. As a result, the loss can be reduced, and the Q_0 of the SWGMR will increase. In this Letter, we use trapezoidal silicon pillars to create an asymmetric effective index profile for the pre-distortion compensation.

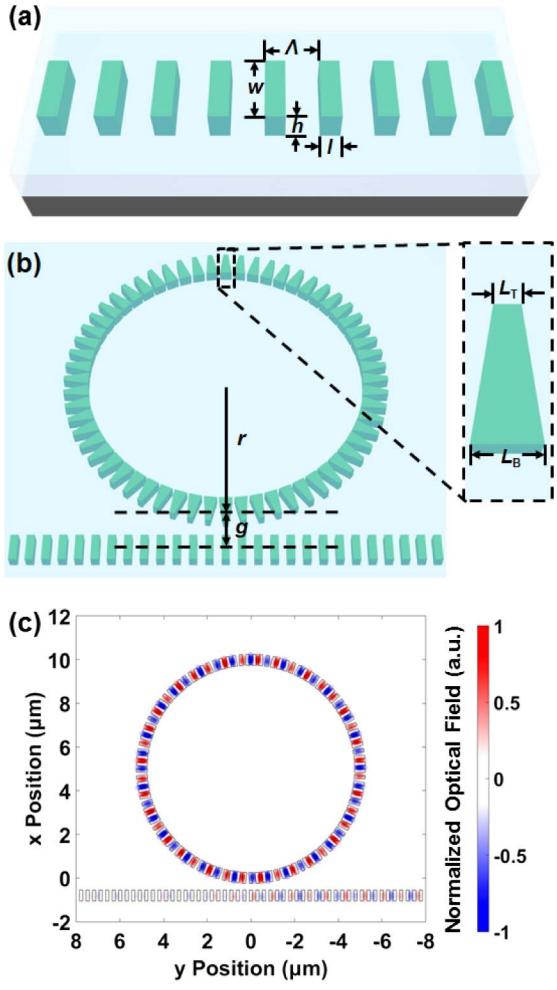

Fig. 1. (a) 3D schematic of a typical SWG waveguide. (b) 3D schematic of a typical T-SWGMR. (c) Typical top view of the optical field of a T-SWGMR on resonance.

The 3D schematic of an SWGMR with trapezoidal silicon pillars (T-SWGMR) is shown in Fig. 1(b), where r and g denote the radius of the T-SWGMR and the center-to-center gap between the SWG bus waveguide and the curved SWG waveguide, respectively. Compared to a conventional SWGMR with rectangular silicon pillars (R-SWGMR), the T-SWGMR is built with trapezoidal silicon pillars to increase its Q_0, while the SWG bus waveguide is still built with rectangular silicon pillars with the aforementioned geometry. As shown in Fig. 1(b), the trapezoidal silicon pillars have two characteristic parameters, top base L_T (at the outer circumference of SWGMRs) and bottom base L_B (at the inner circle of SWGMRs), which could be strategically tuned for the optimized asymmetric effective index profile to minimize bend loss. As the conformal transformation method which is based on 2D approximation can hardly provide a satisfactory quantitative result, especially for SWG waveguides which need to be approximated as strip waveguides first, the 3D finite-difference time-domain (FDTD) method is adopted in the tuning process to optimize the L_T and L_B to realize minimized bend loss. All simulations are performed with the software FullWAVE (Synopsys Inc.). It is found that a trapezoidal silicon pillar with $L_T = 140$ nm and $L_B = 210$ nm could minimize the bend loss to 0.192 dB per 90° bend, which is only 50.1% of the loss of an SWG waveguide bend built with conventional rectangular silicon pillars (0.383 dB per 90° bend).

We design our 5 μm radius T-SWGMRs based on the optimally tuned trapezoidal silicon pillars ($L_T = 140$ nm, $L_B = 210$ nm, $h = 250$ nm and $w = 500$ nm). In order to compare with the results from other groups, 10 μm radius T-SWGMRs are also designed. A control group of 5 μm radius and 10 μm radius R-SWGMRs are also prepared for comparison. To validate that the coupling between the curved SWG waveguide built with trapezoidal silicon pillars and the straight SWG waveguide (the bus waveguide) built with rectangular silicon pillars can be successfully triggered in a T-SWGMR, we simulated T-SWGMRs with various g values by using the 3D FDTD method. Figure 1(c) shows a typical top view of the simulated optical field (Re[Hz]) of a T-SWGMR ($r = 5$ μm and $g = 800$ nm) on resonance. For experimental demonstrations, we fabricated the aforementioned four types of SWGMRs (5 μm radius T-SWGMR, 5 μm radius R-SWGMR, 10 μm radius T-SWGMR, and 10 μm radius R-SWGMR) and measured their transmission spectra. To ensure the critical coupling could be successfully triggered, we applied a parameter scan of the gap size in the fabrication.

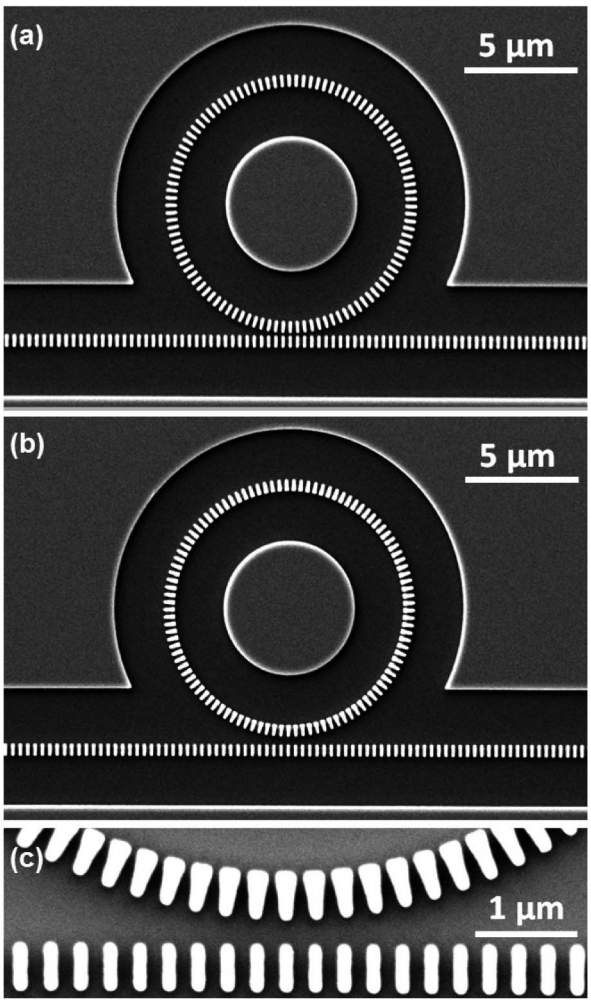

Fig. 2. Scanning electron microscopy (SEM) images of (a) 5 μm radius R-SWGMR and (b) 5 μm radius T-SWGMR. (c) High magnification SEM image of the coupling region of a 5 μm radius T-SWGMR.

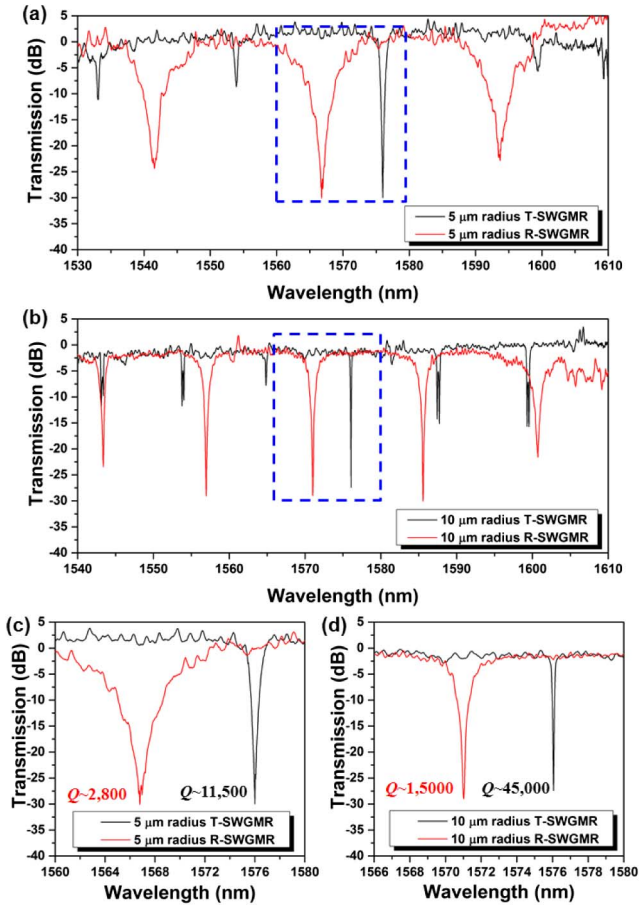

Fig. 3. Full range transmission spectra of (a) 5 μm radius T-SWGMR and R-SWGMR and (b) 10 μm radius T-SWGMR and R-SWGMR. Magnified transmission spectra of (c) 5 μm radius T-SWGMR and R-SWGMR and (d) 10 μm radius T-SWGMR and R-SWGMR, which are around the resonance peaks with the highest quality factors [the blue dashed squares in (a) and (b)].

All devices are fabricated on SOI (Soitec) chips with a 250 nm thick top silicon layer and a 3 μm thick buried oxide (BOX) layer. All structures are patterned in a single E-beam lithography (JEOL 6000 FSE) process in the nanofabrication center at the University of Texas at Austin. The patterns are then transferred to the silicon layer through reactive-ion-etching (PlasmaTherm 790). The SU-8 2005 (MicroChem Corp.) is spin-coated at 3000 rpm to form a 5 μm thick top cladding. An overnight baking at 80°C is applied to reflow the SU-8 for a thorough infiltration [29] and a reduction of scattering loss. Figures 2(a) and 2(b) are the scanning electron microscopy (SEM) images of a 5 μm radius R-SWGMR and a 5 μm radius T-SWGMR, respectively. Figure 2(c) is the high magnification SEM image of the coupling region between the bus waveguide and the micro-ring of a 5 μm radius T-SWGMR.

After spin-coating the SU-8 cladding, the devices are tested in a customized grating coupler alignment system, which has been employed in our previous work [30]. Light from a broadband amplified spontaneous emission (ASE) source (1530–1610 nm, ASE-FL7001P, Thorlabs Inc.) is coupled into the devices through high efficiency SWG couplers [31]. After passing through the devices, light is coupled out and fed into an optical spectrum analyzer (OSA) to obtain the transmission spectra. Figures 3(a) and 3(b) show the wide range transmission spectra of the four types of SWGMRs after subtracting the contribution of grating couplers. Figures 3(c) and 3(d) show the magnified pictures of the resonance peaks with the highest quality factor [the blue dashed squares in Figs. 3(a) and 3(b)]. Both the 5 μm radius and the 10 μm radius T-SWGMR show greatly enhanced quality factors compared with the R-SWGMRs of the same radius. The 5 μm radius T-SWGMR ($g = 780$ nm) has a resonance peak with a quality factor as high as 11,500, which is 4.6 times that of the highest quality factor (~2800) obtained from the 5 μm radius R-SWGMR ($g = 570$ nm). For the 10 μm radius ring, the T-SWGMR ($g = 1020$ nm) has a resonance peak with a quality factor as high as 45,000, which is 3 times that of the highest quality factor ($\sim 15,000$) obtained from the 10 μm radius R-SWGMR ($g = 870$ nm).

The propagation loss α in a ring resonator can be calculated by $\alpha = \lambda/(Q_0 \cdot r \cdot \mathrm{FSR})$ [32], where λ is the wavelength, Q_0 is

Table 1. Measured Propagation Loss

Device Type	$r = 5\ \mu m$ T-SWGMR	$r = 5\ \mu m$ R-SWGMR	$r = 10\ \mu m$ T-SWGMR	$r = 10\ \mu m$ R-SWGMR
α (dB/cm)	16.78	90.44	6.07	15.19

the intrinsic quality factor, r is the radius, and FSR is the free spectral range. The measured propagation loss is summarized in Table 1. For 5 μm radius SWGMRs, one can find that the propagation loss of the T-SWGMR is only 18.6% of the R-SWGMR. This result is smaller than the simulation prediction of 50.1%. The discrepancy can be mainly attributed to the bend mode in the R-SWGMR expanding more in space than the one in the T-SWGMR. Therefore it suffers more loss from the sidewall roughness scattering and material absorption. We want to point out that for T-SWGMRs, only the resonance peak around 1576 nm shows a decent extinction ratio. As R-SWGMRs did not show the same phenomenon, it should be attributed to the asymmetric SWG waveguide couplers built with tuned and non-tuned silicon pillars that are highly dispersive [see Fig. 2(c)]. The highly dispersive couplers in the T-SWGMRs could be further engineered to fabricate critical coupling-based sensors, which have been demonstrated for slot waveguide-based micro-ring resonators [33].

In conclusion, we implemented a geometrical tuning method into SWGMRs and have achieved high quality factor T-SWGMRs. For the first time to the best of our knowledge, we demonstrated the smallest (5 μm radius) T-SWGMR with an applicable quality factor as high as 11,500, 4.6 times higher compared to 5 μm radius R-SWGMR (quality factor ~2800). The quality factor can be increased to 45,000 for a 10 μm radius T-SWGMR, 3 times higher compared with 10 μm radius R-SWGMR (quality factor ~8800) [22]. Geometrically optimized T-SWGMRs have been proven to effectively reduce bend loss and substantially improve quality factors. This study offers a new way to manipulate light-matter interactions in photonic devices.

†These authors contributed equally to this work.

Funding. U.S. Department of Energy (DOE) (DE-SC0013178).

REFERENCES

1. W. Bogaerts, R. Baets, P. Dumon, V. Wiaux, S. Beckx, D. Taillaert, B. Luyssaert, J. Van Campenhout, P. Bienstman, and D. Van Thourhout, J. Lightwave Technol. **23**, 401 (2005).
2. T. Tsuchizawa, K. Yamada, H. Fukuda, T. Watanabe, J. Takahashi, M. Takahashi, T. Shoji, E. Tamechika, S. Itabashi, and H. Morita, IEEE J. Sel. Top. Quantum Electron. **11**, 232 (2005).
3. R. Soref, IEEE J. Sel. Top. Quantum Electron. **12**, 1678 (2006).
4. M. Hochberg, N. C. Harris, R. Ding, Y. Zhang, A. Novack, Z. Xuan, and T. Baehr-Jones, IEEE Solid State Circuits Mag. **5**(1), 48 (2013).
5. H. Subbaraman, X. C. Xu, A. Hosseini, X. Y. Zhang, Y. Zhang, D. Kwong, and R. T. Chen, Opt. Express **23**, 2487 (2015).
6. W. Bogaerts, P. De Heyn, T. Van Vaerenbergh, K. De Vos, S. K. Selvaraja, T. Claes, P. Dumon, P. Bienstman, D. Van Thourhout, and R. Baets, Laser Photon. Rev. **6**, 47 (2012).
7. B. E. Little, S. T. Chu, H. A. Haus, J. Foresi, and J. P. Laine, J. Lightwave Technol. **15**, 998 (1997).
8. F. N. Xia, M. Rooks, L. Sekaric, and Y. Vlasov, Opt. Express **15**, 11934 (2007).
9. F. N. Xia, L. Sekaric, and Y. Vlasov, Nat. Photonics **1**, 65 (2007).
10. V. R. Almeida, C. A. Barrios, R. R. Panepucci, and M. Lipson, Nature **431**, 1081 (2004).
11. P. Dong, S. F. Preble, and M. Lipson, Opt. Express **15**, 9600 (2007).
12. H. Wen, O. Kuzucu, T. G. Hou, M. Lipson, and A. L. Gaeta, Opt. Lett. **36**, 1413 (2011).
13. Q. F. Xu, B. Schmidt, S. Pradhan, and M. Lipson, Nature **435**, 325 (2005).
14. B. G. Lee, B. A. Small, K. Bergman, Q. F. Xu, and M. Lipson, Opt. Lett. **31**, 2701 (2006).
15. Q. F. Xu, B. Schmidt, J. Shakya, and M. Lipson, Opt. Express **14**, 9430 (2006).
16. Q. F. Xu, S. Manipatruni, B. Schmidt, J. Shakya, and M. Lipson, Opt. Express **15**, 430 (2007).
17. A. L. Washburn, L. C. Gunn, and R. C. Bailey, Anal. Chem. **81**, 9499 (2009).
18. M. Iqbal, M. A. Gleeson, B. Spaugh, F. Tybor, W. G. Gunn, M. Hochberg, T. Baehr-Jones, R. C. Bailey, and L. C. Gunn, IEEE J. Sel. Top. Quantum Electron. **16**, 654 (2010).
19. Y. Z. Sun and X. D. Fan, Anal. Bioanal. Chem. **399**, 205 (2011).
20. P. J. Bock, P. Cheben, J. H. Schmid, J. Lapointe, A. Delage, S. Janz, G. C. Aers, D. X. Xu, A. Densmore, and T. J. Hall, Opt. Express **18**, 20251 (2010).
21. V. Donzella, A. Sherwali, J. Flueekiger, S. T. Fard, S. M. Grist, and L. Chrostowski, Opt. Express **22**, 21037 (2014).
22. J. J. Wang, I. Glesk, and L. R. Chen, Opt. Express **22**, 15335 (2014).
23. V. Donzella, A. Sherwali, J. Flueckiger, S. M. Grist, S. T. Fard, and L. Chrostowski, Opt. Express **23**, 4791 (2015).
24. C. Manolatou, M. Khan, S. Fan, P. R. Villeneuve, H. Haus, and J. Joannopoulos, IEEE J. Quantum Electron. **35**, 1322 (1999).
25. M. Soltani, S. Yegnanarayanan, Q. Li, and A. Adibi, IEEE J. Quantum Electron. **46**, 1158 (2010).
26. F. Ladouceur and P. Labeye, J. Lightwave Technol. **13**, 481 (1995).
27. G. Hocker and W. K. Burns, Appl. Opt. **16**, 113 (1977).
28. M. Heiblum and J. H. Harris, IEEE J. Quantum Electron. **11**, 75 (1975).
29. C.-J. Yang, N. Tang, H. Yan, S. Chakravarty, D. Li, and R. Chen, in *Conference on Lasers and Electro-Optics (CLEO)* (Optical Society of America, 2015), paper STu4K.5.
30. Z. Wang, H. Yan, S. Chakravarty, H. Subbaraman, X. C. Xu, D. L. Fan, A. X. Wang, and R. T. Chen, Opt. Lett. **40**, 1563 (2015).
31. X. C. Xu, H. Subbaraman, J. Covey, D. Kwong, A. Hosseini, and R. T. Chen, Appl. Phys. Lett. **101**, 031109 (2012).
32. A. Griffith, J. Cardenas, C. B. Poitras, and M. Lipson, Opt. Express **20**, 21341 (2012).
33. W. Zhang, S. Serna, X. Le Roux, L. Vivien, and E. Cassan, Opt. Lett. **41**, 532 (2016).